

Photocatalytic Degradation of Malathion Using Hydroxyapatite Derived from *Chanos chanos* and *Pangasius dory* Bones [†]

Allen Credo, Mckenneth Pascual, Mark Jerome Villagracia, Alden Villaruz, Erison Roque, Edgar Clyde R. Lopez * and Rugi Vicente C. Rubi *

Chemical Engineering Department, Adamson University, 900 San Marcelino St., Ermita, Manila, Philippines; credoallen@gmail.com (A.C.); kenneth.pascual0987@gmail.com (M.P.); villagracia_markjerome@yahoo.com (M.J.V.); alden_villaruz@gmail.com (A.V.); erison.roque@adamson.edu.ph (E.R.)

* Correspondence: edgarclydelopez09@gmail.com (E.C.R.L.); rugi.vicente.rubi@adamson.edu.ph (R.V.C.R.)

† Presented at the 2nd International Electronic Conference on Processes: Process Engineering—Current State and Future Trends, Online, 17–31 May 2023; Available online: <https://ecp2023.sciforum.net/>.

Abstract: Farmers widely use malathion, even in households, and significant amounts of seep through groundwater and effluent wastewater. It is toxic to animal and human life. Hence its removal from wastewater is necessary. Here, we report the applicability of hydroxyapatite as a catalyst in the UV-light-assisted degradation of malathion. The hydroxyapatite was synthesized via calcination from milkfish (MF1000) and cream dory (CD1000) bones. FTIR and PXRD results proved the successful synthesis of hydroxyapatite from the fish bones. SEM images revealed that the synthesized hydroxyapatite varies from 19 to 52 nm in size with a pseudo-spherical morphology. Degradation efficiency increases when catalyst dosage or irradiation time is increased. Degradation efficiencies range from 8.18% to 67.80% using MF1000 and from 20.50% to 67.90% using CD1000. Malathion obeys the first-order kinetics with a kinetic constant up to $7.0289 \times 10^{-3} \text{ min}^{-1}$ for 0.6 g catalyst loading. Meanwhile, malathion obeys second-order kinetics with a kinetic constant up to $1.1946 \times 10^{-3} \text{ L min}^{-1} \text{ mg}^{-1}$ for 0.6 g loading. Across all catalyst loadings, CD1000 has faster degradation kinetics compared to MF1000. The results of this study validate that the calcined fish bones are effective in removing malathion in an aqueous solution, which significantly impacts lessening the detrimental effects of pesticides in groundwater and wastewater.

Keywords: malathion; photocatalysis; hydroxyapatite; wastewater

Citation: Credo, A.; Pascual, M.; Villagracia, M.J.; Villaruz, A.; Roque, E.; Lopez, E.C.R.; Rubi, R.V.C. Photocatalytic Degradation of Malathion Using Hydroxyapatite Derived from *Chanos chanos* and *Pangasius dory* Bones. *Eng. Proc.* **2023**, *37*, x. <https://doi.org/10.3390/xxxxx> Published: 17 May 2023



Copyright: © 2023 by the authors. Submitted for possible open access publication under the terms and conditions of the Creative Commons Attribution (CC BY) license (<https://creativecommons.org/licenses/by/4.0/>).

1. Introduction

The consumption of agrochemicals in the Philippines is relatively large due to the massive farming activities in the country. Agrochemicals such as fertilizers and pesticides are used to boost production, ensure productivity and prevent crop damage. Despite its benefits in elongating the lives of crops through the prevention of pests, pesticides are poisonous to insects and humans. Since these chemicals have been occurring for decades, consequences emerge, such as contamination of water sources and indirect harm to human health [1]. Fungicides such as dithane, mancozeb, and funguran, insecticides such as cypermethrin, malathion, and decis, and weedicides such as clear out and round up were found to be the pesticides that are most consumed by Filipino farmers [1,2]. Brought about by the large consumption of the said pesticides, some of these have been found in bodies of water. Specifically, cyhalothrin, cypermethrin, deltamethrin were detected on streams and rivers in the islands of Leyte [3]. Organochlorine pesticides such as dieldrin, endosulfan II, α -Hexachlorocyclohexane, and heptachlor are detected in the surface water and groundwater in Pampanga [4]. Additionally, catchments along Laguna Lake have also been proven to be positive in terms of pesticide contamination due to agricultural

activities done around the area [5]. Presently, pesticide contamination in bodies of water and wastewater are of high concern as current wastewater treatment methods are somehow inefficient in removing such hazardous chemicals.

To prevent further damages brought about by pesticide contamination of water streams, one solution is the treatment of such wastewater prior to final disposal which leads to the high demand of technologies for the removal of pesticides from agricultural run-offs and wastewater [6]. Among these treatment are electrochemical methods [7], adsorption [8], phytoremediation [9], and photocatalysis [10]. Among these, photocatalysis remain the top choice of researchers due to its simplicity in completely degrading the pollutants. In photocatalysis, the system is irradiated by light to induce electron and holes formation on the catalyst's surface. These electron holes would then function as a mediator of redox reaction. The end product would then react with dissolved contaminants in the water which would follow the degradation or separation of the contaminant with water [11]. A wide range of photocatalysts have been investigated for pesticide degradation such as TiO_2 [12], ZnO , [13], and other semiconductors [14], among others.

Recently, the use of greener photocatalysts such as hydroxyapatite (HAp, $\text{Ca}_{10}(\text{PO}_4)(\text{OH})_2$) for photocatalysis have been studied to replace conventional semiconducting photocatalysts [15]. Hydroxyapatite has been proven to degrade, via photocatalysis, dyes [16], pharmaceuticals [17], and pesticides [18] from wastewater and aqueous solutions.

Here we report the synthesis of HAp from the fish bones of milkfish, *Chanos chanos*, and cream dory, *Pangasius dory*, via calcination. The fish bones—derived HAp were then used for the photocatalytic degradation of malathion in aqueous solutions. We investigated the effect of catalyst loading, UV light irradiation time, and HAp type on the degradation of malathion.

2. Materials and Methods

2.1. Materials

The milkfish bones were obtained from Limay, Bataan. The cream dory bones were obtained from Libertad Public Market. 100 mg of Malathion Pestanal ($\text{C}_{10}\text{H}_{19}\text{O}_6\text{PS}_2$, 98%, Belman Laboratories) was diluted with 1.0 L of deionized water to produce the simulated malathion-contaminated water.

2.2. Synthesis and Characterization of Hydroxyapatite

The fish bones of the milkfish and cream dory were cleaned separately in boiling water to remove any impurities such as meat, fats, scales, and any other contaminants. The fish bones were then subjected to convection air drying at 40 °C. Then, the fish bones were cut into 20–30 mm sections. The fish bones were subjected to calcination (EYELA TMF-2200) at 1000 °C for 2 h. The milkfish and cream dory bones were calcined separately. The HAp derived from milkfish bones was named MF1000, and the HAp derived from cream dory bones was named CD1000.

The structure of the fish bone-derived HAp was characterized via powder X-ray diffraction (PXRD, Shimadzu XRD-7000 Maxima-X; 40 kV; 30 mA) with $\text{CuK}\alpha$ radiation. The morphology of the fish bones derived from hydroxyapatite was evaluated via scanning electron microscopy with energy dispersive x-ray analysis (SEM-EDX, JEOL 5300). The functional groups on the synthesized powders were determined using a Fourier infrared transform spectroscopy (FTIR, Perkin Elmer Spectrum Two L60000A).

2.3. Photocatalytic Degradation of Malathion

A simulated aqueous malathion solution was prepared by dissolving 100 mg of malathion in 1.0 L deionized water, resulting in an initial concentration of 100 ppm. For the photocatalytic degradation, a homemade photocatalytic reactor box was made, and a UV lamp ($\lambda_{\text{max}} = 254 \text{ nm}$; Sankyo Denki, Hiratsuka, Japan) was installed in the photoreactor

box. The lamp was positioned horizontally and 10 cm above the surface of the solution. The box's interior was covered with aluminum foil to prevent outside light's passage into the box. 0.2 g of the hydroxyapatite catalyst was added to the solution before UV irradiation. A magnetic stirrer was also installed on the reactor to maintain adsorption equilibrium between the hydroxyapatite catalyst and the Malathion solution. The solution was kept at room temperature. The solution was irradiated for 30, 60, 90, 120, and 150 min. Following this, the malathion absorbance on the filtrate was determined using a UV-Vis spectrophotometer (Lambda 25 L60000B UV-Visible Perkin Elmer, 190–1100 nm) measured at 210 nm. The malathion's wavelength was adopted from Sharma (2016). The degradation efficiency was expressed in terms of the initial and final concentration and was estimated using the equation below:

$$\% \text{ degradation} = \frac{C_0 - C}{C_0} \times 100, \quad (1)$$

where C_0 is the concentration at 0 min, and C is the variable concentration (concentration at the time of withdrawal of sample). The same process was repeated using 0.4 g and 0.6 g of hydroxyapatite to determine the effect of the catalyst dosage on the degradation efficiency. The hydroxyapatite from the milkfish bones and cream dory bones was used as a photocatalyst separately.

3. Results

3.1. Characterization of Hydroxyapatite

The morphology of the hydroxyapatite was analyzed using a Scanning Electron Microscope. Both samples derived from the two fishes appear to be pseudospherical. Figure 1a shows the SEM image for the cream dory-derived hydroxyapatite with particle size ranging from 19 nm to 43 nm. The milkfish-derived hydroxyapatite's SEM image is shown in Figure 1b, with particle sizes ranging from 26 to 52 nm. The HAp particles appear clustered together because of moisture content which causes the powder particles to stick together. Nevertheless, the composition of the CD1000 and MF1000 are almost identical.

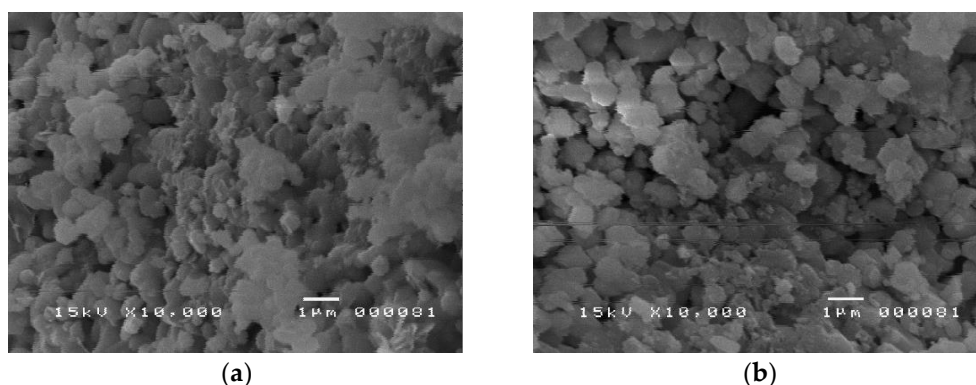


Figure 1. Surface morphology of (a) Cream dory-derived Hydroxyapatite and (b) Milkfish-derived hydroxyapatite.

The FTIR spectra of CD1000 and MF1000, shown in Figure 2a, prove that numerous functional groups are present in the HAp samples. The peak around 3500 cm^{-1} may be attributed to -OH vibrations brought about by the moisture adhering to the powders. Peaks at around 1430 cm^{-1} and 1520 cm^{-1} correspond to C=O stretching could be linked to CO_2 adsorbed on the sample surface during testing. The peaks at about 550 and 600 cm^{-1} are more likely due to the vibrational modes of the phosphate group in the apatite.

Figure 2b shows the PXRD results of CD1000 and MF1000, which were compared to a standard hydroxyapatite reference. Both CD1000 and MF1000 have similar peaks, indicating similar crystal structure of the two HAp powders. The major peaks for the milkfish-

derived catalyst were at 31.97°, 33.10°, and 32.38° while the cream dory-derived catalyst had 31.91°, 33.04°, and 32.32° as its peaks. All peaks observed are evidence that a typical hydroxyapatite was produced from both fish bones compared to a standard reference (JCPDS: 09-0432).

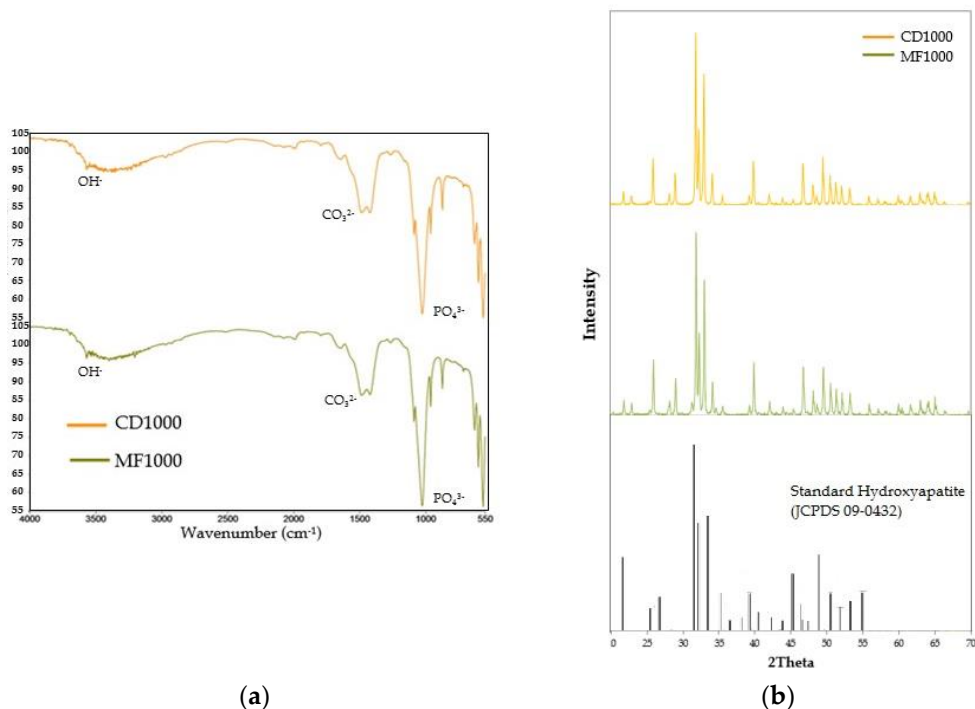


Figure 2. (a) FTIR spectra and (b) X-ray diffraction profiles of cream dory-derived Hydroxyapatite (CD1000) and Milkfish-derived Hydroxyapatite (MF1000).

3.2. Photocatalytic Degradation of Malathion

As shown in Figure 3, the degradation efficiency of malathion increases with an increase in catalyst dosage and UV exposure time. The highest degradation was reached after 150 min of exposure to UV light with 0.6 g of the catalyst. The highest degradation efficiency obtained for the milkfish-derived catalyst was 67.80%, while the cream-dory-derived catalyst resulted in 67.99% degradation. Both were obtained at 0.6 g of the catalyst and UV light exposure for 150 min. These results may be due to kinetic effects since the catalyst and the pollutant have a longer time to collide and react with each other at longer UV exposure times (Nuengmatcha, 2016). Moreover, increased catalyst loading means more active sites for malathion to react with during its degradation, hence the higher degradation efficiencies.

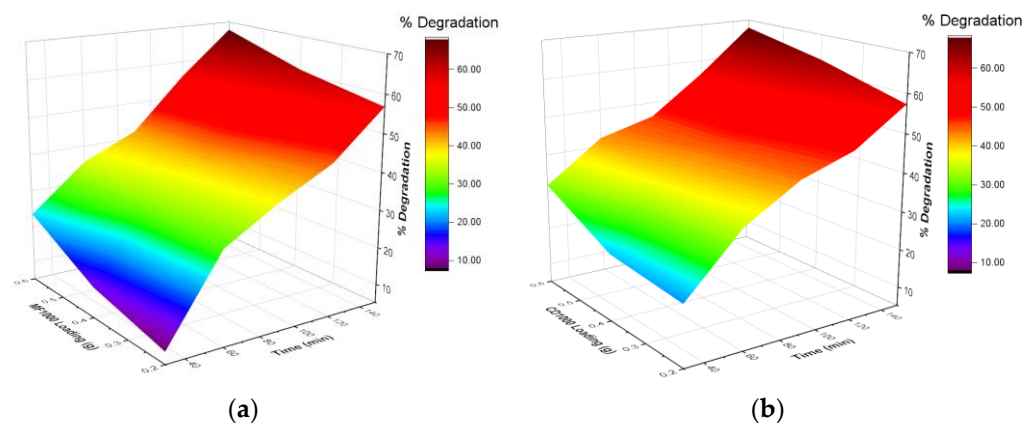


Figure 3. 3D plots for the photocatalytic degradation of malathion under UV light using (a) MF1000 and (b) CD1000 as photocatalysts.

Three-way ANOVA was adopted to determine the significant effect of varying the parameters (catalyst loading, UV exposure time, and catalyst type) on the photocatalytic degradation of malathion. The linear effect of catalyst loading, UV exposure time, and catalyst type all significantly affect the degradation efficiency of malathion. Moreover, it was found that the two-factor interaction between UV exposure time and catalyst loading and between UV exposure time and HAp type also significantly affect the degradation of malathion. Meanwhile, the two-factor interaction between catalyst loading and HAp type has an insignificant impact on malathion degradation.

3.3. Degradation Kinetics

To investigate the mechanism of the malathion degradation, we fitted the experimental data to first-order and second-order kinetics. When MF1000 was used as a photocatalyst, malathion obeys the first-order kinetics with a kinetic constant ranging from $5.2503 \times 10^{-3} \text{ min}^{-1}$ for 0.2 g catalyst loading to $7.0289 \times 10^{-3} \text{ min}^{-1}$ for 0.6 g catalyst loading. Meanwhile, malathion obeys second-order kinetics with a kinetic constant ranging from $0.8520 \times 10^{-3} \text{ L min}^{-1} \text{ mg}^{-1}$ for 0.2 g loading to $1.1946 \times 10^{-3} \text{ L min}^{-1} \text{ mg}^{-1}$ for 0.6 g loading. Across all catalyst loadings, CD1000 has faster degradation kinetics compared to MF1000. More studies are needed to elucidate the mechanism of malathion degradation in water using the synthesized HAp.

4. Conclusions

Hydroxyapatite (HAp) was successfully synthesized via calcination. The HAp produced has a particle size ranging from 19 nm to 52 nm with a pseudo-spherical morphology. PXRD and FTIR analysis confirmed the successful synthesis of HAp. Three-way ANOVA showed that catalyst loading, UV exposure time, and HAp type are significant factors in the photocatalytic degradation efficiency of malathion in water. Moreover, the two-factor interaction between UV exposure time and catalyst loading and between UV exposure time and HAp type affects the degradation efficiency. Kinetic study shows that the degradation mechanism of malathion is best fit in a first-order reaction when using milkfish-derived HAp (MF1000) and in a second-order reaction when using cream dory-derived HAp (CD1000). Overall, CD1000 yielded faster degradation kinetics compared to MF1000.

Author Contributions: Conceptualization, R.V.C.R.; methodology, A.C., M.P., M.J.V., A.V. and R.V.C.R.; software, E.C.R.L.; validation, E.C.R.L. and R.V.C.R.; formal analysis, A.C., M.P., M.J.V., A.V., E.C.R.L. and R.V.C.R.; investigation, A.C., M.P., M.J.V., A.V., E.C.R.L. and R.V.C.R.; resources, E.R. and R.V.C.R.; data curation, A.C., M.P., M.J.V., A.V., E.C.R.L. and R.V.C.R.; writing—original draft preparation, A.C., M.P., M.J.V., and A.V.; writing—review and editing, E.C.R.L., E.R. and R.V.C.R.; visualization, E.C.R.L.; supervision, R.V.C.R.; project administration, E.R. and R.V.C.R.; funding acquisition, E.R. and R.V.C.R. All authors have read and agreed to the published version of the manuscript.

Funding: This research received no external funding.

Institutional Review Board Statement: Not applicable.

Informed Consent Statement: Not applicable.

Data Availability Statement: Not applicable.

Conflicts of Interest: The authors declare no conflict of interest.

References

1. Varca, L.M. Pesticide residues in surface waters of Pagsanjan-Lumban catchment of Laguna de Bay, Philippines. *Agric. Water Manag.* **2012**, *106*, 35–41. <https://doi.org/10.1016/j.agwat.2011.08.006>.
2. Elfman, L.; Tooke, N.E.; Patring, J.D. Detection of pesticides used in rice cultivation in streams on the island of Leyte in the Philippines. *Agric. Water Manag.* **2011**, *101*, 81–87. <https://doi.org/10.1016/j.agwat.2011.09.005>.
3. Navarrete, I.A.; Tee, K.A.M.; Unson, J.R.S.; Hallare, A.V. Organochlorine pesticide residues in surface water and groundwater along Pampanga River, Philippines. *Environ. Monit. Assess.* **2018**, *190*, 289. <https://doi.org/10.1007/s10661-018-6680-9>.
4. Bajet, C.; Kumar, A.; Calingacion, M.; Narvacan, T. Toxicological assessment of pesticides used in the Pagsanjan-Lumban catchment to selected non-target aquatic organisms in Laguna Lake, Philippines. *Agric. Water Manag.* **2012**, *106*, 42–49. <https://doi.org/10.1016/j.agwat.2012.01.009>.
5. Saleh, I.A.; Zouari, N.; Al-Ghouthi, M.A. Removal of pesticides from water and wastewater: Chemical, physical and biological treatment approaches. *Environ. Technol. Innov.* **2020**, *19*, 101026. <https://doi.org/10.1016/j.eti.2020.101026>.
6. Trellu, C.; Vargas, H.O.; Mousset, E.; Oturan, N.; Oturan, M.A. Electrochemical technologies for the treatment of pesticides. *Curr. Opin. Electrochem.* **2021**, *26*, 100677. <https://doi.org/10.1016/j.coelec.2020.100677>.
7. Ho, S. Low-Cost Adsorbents for the Removal of Phenol/Phenolics, Pesticides, and Dyes from Wastewater Systems: A Review. *Water* **2022**, *14*, 3203. <https://doi.org/10.3390/w14203203>.
8. Karthikeyan, R.; Davis, L.C.; Erickson, L.E.; Al-Khatib, K.; Kulakow, P.; Barnes, P.L.; Hutchinson, S.; Nurzhanova, A.A. Potential for Plant-Based Remediation of Pesticide-Contaminated Soil and Water using Nontarget Plants such as Trees, Shrubs, and Grasses. *Crit. Rev. Plant Sci.* **2004**, *23*, 91–101. <https://doi.org/10.1080/07352680490273518>.
9. Bruckmann, F.S.; Schnorr, C.; Oviedo, L.R.; Knani, S.; Silva, L.F.O.; Silva, W.L.; Dotto, G.L.; Rhoden, C.R.B. Adsorption and Photocatalytic Degradation of Pesticides into Nanocomposites: A Review. *Molecules* **2022**, *27*, 6261. <https://doi.org/10.3390/molecules27196261>.
10. Zeshan, M.; Bhatti, I.A.; Mohsin, M.; Iqbal, M.; Amjed, N.; Nisar, J.; AlMasoud, N.; Alomar, T.S. Remediation of pesticides using TiO₂ based photocatalytic strategies: A review. *Chemosphere* **2022**, *300*, 134525. <https://doi.org/10.1016/j.chemosphere.2022.134525>.
11. Andronic, L.; Leles, M.; Enesca, A.; Karazhanov, S. Photocatalytic activity of defective black-titanium oxide photocatalysts towards pesticide degradation under UV/VIS irradiation. *Surf. Interfaces* **2022**, *32*, 102123. <https://doi.org/10.1016/j.surfin.2022.102123>.
12. Khan, S.H.; Pathak, B. Zinc oxide based photocatalytic degradation of persistent pesticides: A comprehensive review. *Environ. Nanotechnology, Monit. Manag.* **2020**, *13*, 100290. <https://doi.org/10.1016/j.enmm.2020.100290>.
13. Vaya, D.; Surolia, P.K. Semiconductor based photocatalytic degradation of pesticides: An overview. *Environ. Technol. Innov.* **2020**, *20*, 101128. <https://doi.org/10.1016/j.eti.2020.101128>.
14. Rocha, R.L.P.; Honorio, L.M.C.; Bezerra, R.D.d.S.; Trigueiro, P.; Duarte, T.M.; Fonseca, M.G.; Silva-Filho, E.C.; Osajima, J.A. Light-Activated Hydroxyapatite Photocatalysts: New Environmentally-Friendly Materials to Mitigate Pollutants. *Minerals* **2022**, *12*, 525. <https://doi.org/10.3390/min12050525>.
15. Mariappan, A.; Pandi, P.; Rajeswarapalanichamy, R.; Neyvasagam, K.; Sureshkumar, S.; Gatasheh, M.K.; Hatamleh, A.A. Bandgap and visible-light-induced photocatalytic performance and dye degradation of silver doped HAp/TiO₂ nanocomposite by sol-gel method and its antimicrobial activity. *Environ. Res.* **2022**, *211*, 113079. <https://doi.org/10.1016/j.envres.2022.113079>.
16. Zhang, Y.; Wang, L.; Lu, L.; Liu, M.; Yuan, Z.; Yang, L.; Liu, C.; Huang, S.; Rao, Y. Highly efficient decontamination of tetracycline and pathogen by a natural product-derived Emodin/HAp photocatalyst. *Chemosphere* **2022**, *305*, 135401. <https://doi.org/10.1016/j.chemosphere.2022.135401>.
17. Rubi, R.V.; Roque, E.; Rosa, F.D.; Estoque, R.M.; Olvido, G.; Perey, P.J.; Teresa, J.S.; Tesalona, M.A. Photocatalytic degradation of Atrazine herbicide using nano-Hydroxyapatite from Cow Bone synthesized via Simulated Body Fluid. *IOP Conf. Series: Mater. Sci. Eng.* **2020**, *778*, 012013. <https://doi.org/10.1088/1757-899x/778/1/012013>.

Disclaimer/Publisher's Note: The statements, opinions and data contained in all publications are solely those of the individual author(s) and contributor(s) and not of MDPI and/or the editor(s). MDPI and/or the editor(s) disclaim responsibility for any injury to people or property resulting from any ideas, methods, instructions or products referred to in the content.